Journal of Applied Sciences, Information and Computing
Volume 6, Issue 1, April-May 2025
School of Mathematics and Computing, Kampala International University

ISSN: 1813-3509 **https://doi.org/10.59568/JASIC-2025-6-1-19**

The Solid-State Characteristics of ZnS Thin Films Grown by CBD Technique

***Babatunde Rasaq Ayinla[1,2], Odunaike Rasaki Kola [1], Laoye John Abidemi[1]**
[1] Department of Physics, Olabisi Onabanjo University, Ago-Iwoye, Nigeria
[2] Department of Science Laboratory Technology, Federal Polytechnic Ilaro, Nigeria
[*]Email: rasaq.bababtunde@federalpolyilaro.edu.ng

Abstract
ZnS thin films were coated onto fluorine doped tin oxide glass substrates using chemical bath deposition technique. The bath solution was made from 0.1 M of zinc nitrate and thiourea as the source of zinc and sulphur ions, respectively. The precursor solution temperature was kept at 70°C and the time of deposition was varied between 5 and 30 min. The impact of time of deposition was then examined on some solid state characteristics of the films. The structural properties such as crystallite size, micro lattice strain and dislocation density were examined using x-ray diffractometer. The morphological and compositional features were studied using scanning electron microscopic and energy dispersive spectroscopic. The optical characteristics were measured with Uv vis spectrophotometry. The investigation showed that some films were amorphous and some had polycrystalline structure, the films were rough, dense and covered the substrates, the compositional analysis confirmed the presence of zinc, sulphur and oxygen. The optical analysis showed that the films had high bandgap between 3.79 and 3.97 eV.
Keywords: Bandgap, solid-state, time, zinc nitrate

1. Introduction
A larger percentage of the global energy supply came from convectional energy mains coal, natural gas and oil as examples. Nevertheless, these convectional energy sources cannot satisfy the increased huma energy consumption (Netravati, & Patil, 2015; Rajapakse, 2007) There are several alternatives to convectional energy sources these include, hydrothermal, biomass, wind and solar energy (Kowsar et al., 2019).
Solar energy is most reliable among the alternative energy sources because its energy is fuelled by the sun which releases a huge quantity of energy manifested as heat and radiation at no cost (Sharma et al., 2015) . The sun radiations can be converted to electrical energy by photovoltaic materials or solar cells. A photovoltaic device is a p-n junction material, when light energy with larger than or equivalent to the band gap of light absorbing layer impinge on the photovoltaic device, electrons are moved to the conduction band from the valence band in the absorbing material (Fluieraru et al., 2019).When a pair of photons are created, the negative charge carriers cross the junction and move from n to the p region while the positive charge carriers go from the p to the n region, liberating their energy before combining with each other again (Chander et al., 2015).

Cu(In, GA)Se_2 as an absorber component thin film photovoltaic cells employs cadmium sulphide as its buffer component and demonstrated at least 20% efficiency. However, cadmium is poisonous and has major negative effects on the ecosystem (Wei et al., 2013) ZnS thin film has been considered as the best binary compound semiconducting material to replace the toxic CdS because to its superior qualities, including its high refractive index (2.35), dielectric constant, and wide band gap (3.7 eV) (Manjulavalli & Kannan, 2015).

The films have been coated using different techniques, such as evaporation (Kumar & Mahesh, 2017; Vishwakarma, 2015), radio frequency sputtering (Haque et al., 2014; Hwang et al., 2012), spray pyrolysis (Al-diabat et al., 2019; Suhail & Ahmed, 2014), spin coating (Osanyinlusi, 2020), successive ionic layer adsorption and reaction (SILAR) (Djelloul et al., 2016) and chemical bath deposition (CBD) (Abdullah et al., 2012; Ahn & Um, 2015; Al-diabat et al., 2019; Nabiyouni et al., 2011; Shinde et al., 2011). Among these techniques, CBD is the mostly adopted method to grow ZnS thin films due to its unique advantages over other methods. These advantages are efficiency, cost-effectiveness and large-scale capability. However, several parameters such pH of precursor solution, temperature of deposition, concentration of precursor solution and time of deposition can be studied on the properties of the films. In this study, influence of time of deposition on solid state properties of the films is investigated.

2. Materials And Method

The deposition of ZnS thin films was done on fluorine doped tin oxide (FTO) glass substrates. Before the deposition, the substrates were ultrasonically cleaned in acetone and deionized water for 15 minutes each, rinsed with deionized water and they were finally dried in an oven at 40ºC. The chemical bath was formed by adding 30 mL of ($Zn(NO_3)_2$ at 0.1 M and 15 ml of triethanolamine at 2.9 M in a 100 ml beaker. The solution was milky initially and after stirring it for 30 minutes at 60ºC it became colourless and homogeneous. Then, 30 ml of (CH_4N_2S) at 0.1 M was poured to the precursor and further mixed for 30 minutes. The solution was poured into a 50 ml chromatography tank and five (5) pre-cleaned FTO substrates were vertically placed into the tank, the tank was placed in a water bath at 70ºC. The substrates were allowed to stay in the bath for 5, 10, 15, 20 and 30 minutes, respectively. Thereafter, the substrates were removed and found deposited with milky white deposits. To get rid of extra residues, the samples were rinsed with distilled water.. The films were annealed in an oven (Gen.Lab) at 200ºC for 15 minutes and the thickness of the film was determined by a double-weight method using an analytical balance.

3. Material Characterization

Structural Analysis

The structural characteristics of the films were measured with Pan Analytical Empryrean X-ray diffractometer Tokyo, Japan and configured to generate diffractions using a CuKa radiation set at 40kV and 20mA at a scanning rate of 2-0/min in the 2 to 70º range at room temperature. The films' dislocation density, microstrain (ϵ), and crystallite size (D) were determined according to Debye Scherrer Eqn 1,2 and 3, respectively.

$$D = \frac{k\lambda}{\beta cos\theta} \quad (1)$$

$$\epsilon = \frac{\beta cos\theta}{4} \quad (2)$$

$$\delta = \frac{1}{D^2} \quad (3)$$

where D = crystallite size

k= Scherrer constant with numerical value equals 0.96

λ = wavelength of X ray with numerical value of 1.5406 nm

β = the full width at half maximum height measured in radian

θ = the diffraction angle at the peak

Surface Morphology

Using a JEOL-JSM 7600F scanning electron microscope (SEM) (Japan), the nature of the thin layers at the substrate surface was investigated. A constant 20 kV was used as the accelerating voltage. To enable comparison research into the variations in the composition of the thin films, all of the SEM micrographs were attained at the same magnification.

Compositional Analysis

Energy Dispersive X-ray examination (EDX) was used for the quantitative examination of the films in order to determine the stoichiometry of the thin films. The SEM is connected to this unit. A portion of the incident electrons excite the sample atom when they impact the substrate of the film, and when the atom returns to its ground state, it releases an X-ray. The excited element's atomic number and the X-ray's energy were correlated. An X-ray detector is a lithium-drifted Si-diode kept at liquid nitrogen temperature. JEOL-JSM 7600F Japan was used to analyse the films' compositional characteristics.

Optical Analysis

The Avantex UV visible spectrophotometer was used to measure the thin films' optical transmittance in the wavelength range of 239.534 nm to 999.495 nm. The spectrophotometer provided the film transmittance measurements.

The absorbance (A) was calculated from the percentage transmittance (T) according to Eqn.4

$$A = 2 - logT \quad (4)$$

The absorbance coefficients (α) of the films were calculated according to Eqn. 5.

$$\alpha = \frac{2.303A}{t} \quad (5)$$

where A is absorbance and t is the thickness of the film.

The photon energy (E) was calculated in eV according to Eqn. 6.

$$E = \frac{1243}{\lambda} \quad (6)$$

4. Result And Discussion

4.1 Structural Properties

The XRD patterns of ZnS thin films is presented in Fig.1. The pattern shows that the films deposited for 5, 10, and 20 minutes were amorphous, which showed that the films were highly disordered. The reason for the amorphous nature could be attributed to the low percentage of sulphur in the films composition as revealed by energy dispersive spectroscopy (EDS). A similar amorphous pattern was observed in the ZnS thin films coated by CBD method at varying pH; at pH = 11.5, no diffraction peak was visible (Ben Nasr et al., 2006). Also, no diffraction peak was observed in the ZnS films deposited by a CBD technique at a constant temperature of 80°C at a varying deposition time between 1.5 and 2.5 hours (Zhou et al., 2011). Amorphous structural patterns were also observed in the thin films of ZnS deposited onto glass substrates using the SILAR technique at varying cycles of 10, 20, 30, and 40 (Gułkowski & Krawczak, 2017) .However, the films deposited for 15 and 30 minutes exhibited a polycrystalline structure with six diffraction peaks located at 2θ = 26.42, 33.62, 37.64, 51.42, 61.38, and 65.40°, indexed with (100), (101), (110), (002), (102), and (112), respectively. Though the most prominent peak reflected wurtzite ZnS structure. The pattern that was seen matched the normal JCPDS Card No. 00-001-0677). The average crystallite size and micro lattice strain of polycrystalline ZnS films calculated according to Debye Scherrer Equations 1and 2 respectively. the dislocation density calculated according to Equation 3 as presented in Table 1. The Table shows that the average crystallite of ZnS films deposited for 15 minutes was higher than the films deposited for 30 minutes. The microlattice strain and dislocation density were affected by the crystallite size; the higher the crystallite size, the lower the microlattice strain. The higher percentage of thiourea as the source of sulphur in the films deposited for 15 minutes than films deposited for 30 minutes, as revealed by energy dispersive spectroscopy, may be a factor that caused higher crystallinity in the film. Also, the low strain indicates better lattice arrangement in films deposited for 15 minutes. The values of crystallite size were higher than 8.8 nm when ZnS thin films were spin coated ((Osanyinlusi, 2020) but they were within the calculated crystallite size range between 8 and 130 nm in the thin films of ZnS sprayed by CBD procedure (Kawar & Pawar, 2010))..Also, the results well matched the crystallite size of 117 nm for undoped ZnS thin films (Nikzad et al., 2019).

The connection between absorbance coefficient (α) and incident photon energy ($h\nu$) is shown in Eqn.7

$$\alpha h\nu = A\sqrt{h\nu - E_g} \quad (7)$$

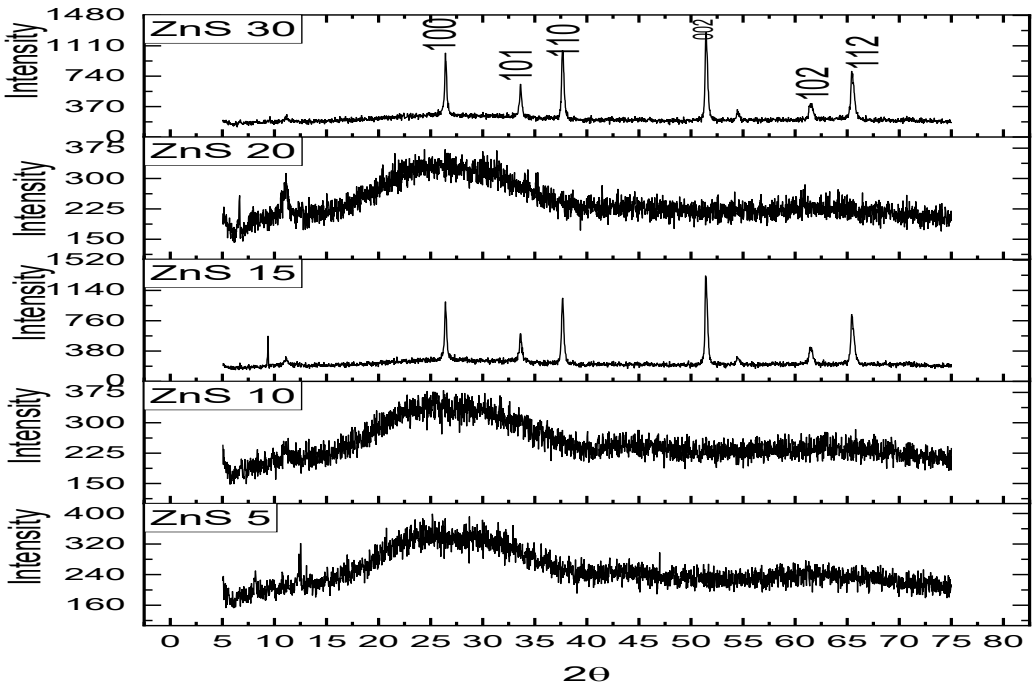

Fig. 1 Structural patterns of ZnS films at varying deposition time

Table 1 Crystallite Size, micro strain and dislocation density of crystalline ZnS thin films

Sample	Crystallite size D (nm)	Micro strain ϵ x 10^{-4}	Dislocation density δ x 10^{14} Line/m^2

ZnS deposited for 15 min.	60. 49	7.08	2.73
ZnS deposited for 30 min	58.20	6.40	2.90

4.2 Surface Morphology

The morphological analysis of ZnS thin films at different times of deposition is presented in Fig. 2 The substrates were covered with films with no cracks. There were some white spots in the SEM patterns that might be colloidal particle sedimentation mixed with ZnS.The film's roughness increased as deposition time increased. The surface roughness increased as the time of deposition enlarged, the rise in film thickness may be an influence. A similar observation was observed in the morphology at surface of ZnS thin films coated at a constant temperature of 80ºC at varying deposition times between 1 and 3 hours. As the deposition time increased, the number of big particles increased (Zhou et al., 2011). However, the films deposited for 15 and 30 minutes showed larger grains with low porosity; evidence of this was observed in the structural properties, which showed that the films deposited for 15 and 30 minutes were polycrystalline while others were amorphous.

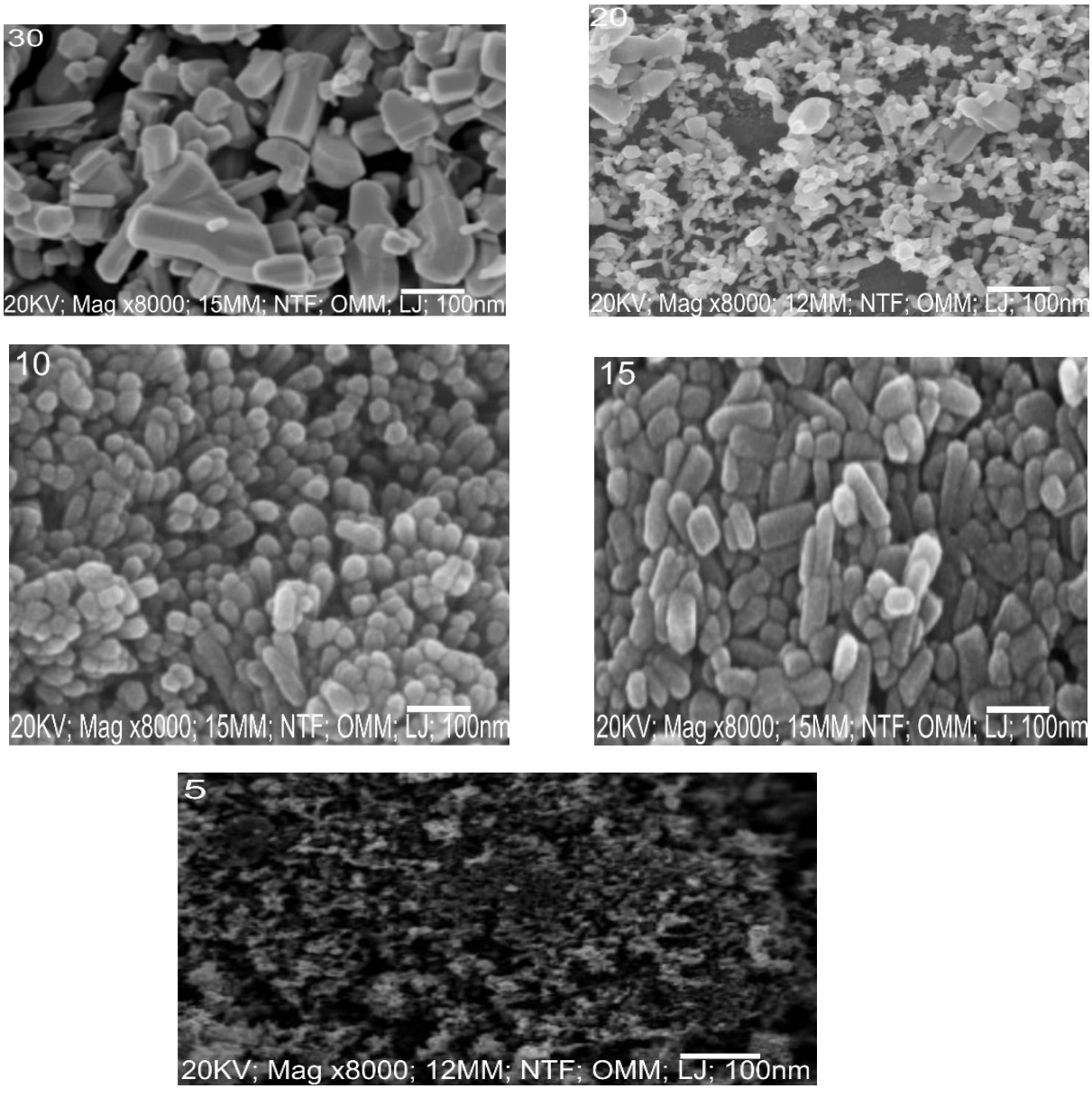

Fig.2: SEM images of ZnS thin films at different deposition times

4.3 Compositional Analysis

Fig. 3 presents the compositional atomic percentage of elements presented in the thin films of ZnS grew at various deposition times, as confirmed EDS. The EDS results displayed that Zn, S, and O were presented in all the samples. The zinc percentage

was higher than the percentage of sulphur in all the films because sulphur has a higher affinity for oxygen, so it could have been transformed to SO_2 and then disappeared. This is established by the presence of oxygen (O) in the EDS analysis. The observation was similar to the EDS results of ZnS films coated by a spin coating method (Osanyinlusi, 2020) .

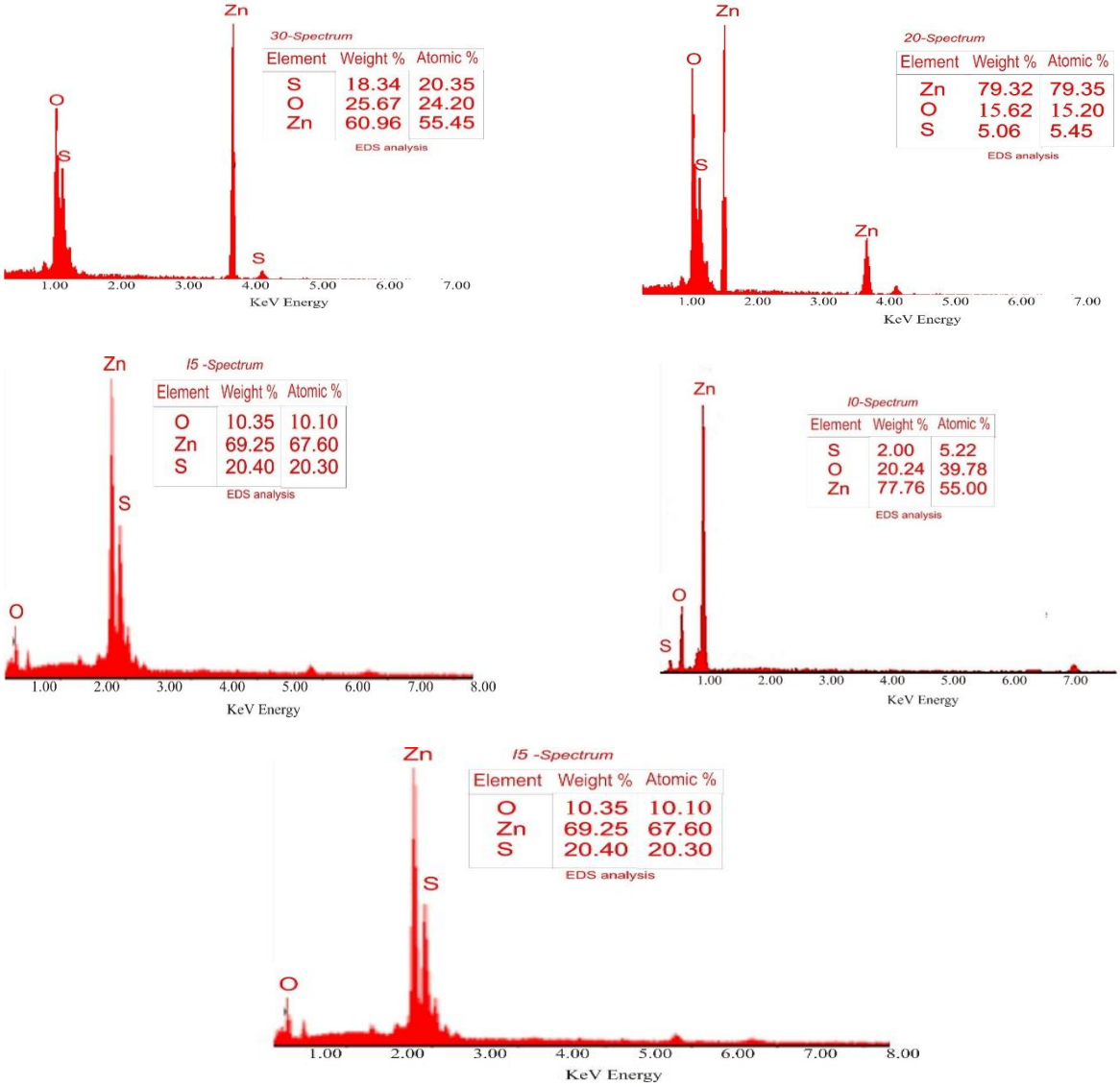

Fig.3. EDS of ZnS different deposition times

4.4 Optical Properties

Optical transmittance spectra

The transmittance spectral of ZnS at varying deposition times is shown Fig 4a. The spectral increases sharply from the UV to visible region of electromagnetic radiation. The ZnS sample deposited for 5 min transmitted between 21.76 and 70.83% measured between 401.75 and 697.04 nm. Samples of films deposited for 10 min had a minimum transmittance of 42.05 % at 401.15 nm and maximum transmittance of 65.38 % at wavelength 697.62nm. The range of transmittance of ZnS films deposited for 15 min was between 28.84 and 90.05% measured between 401.75 and 693.02 nm within the electromagnetic spectrum's visible region. The last sample of ZnS films deposited for 30 minutes showed transmittance between 57.83 and 99.3 % measured between 401.75 and 656.17 nm. From the values of transmittance, it shows that the transmittance of ZnS films increases as time of deposition increases except for the sample deposited for 10 minutes which does not agree with the decrease in transmittance as deposition time increases the reason for this could be attributed to the low percentage of the sulphur in the sample as revealed by the EDX analysis.

4.5 Optical absorbance spectra

The absorbance spectral of ZnS films also decreases as wavelength increases, the absorption was high at ultra-violent range and lower in infrared region as showed in Fig.2b.. The average percentage absorption was measured in the observable part of

 https://doi.org/10.59568/JASIC-2025-6-1-19

electromagnetic radiation. The average absorbances of ZnS deposited for 5, 10, 15, 20 and 30 minutes were 41.20, 31,35, 35.15, 14.40 and 12.30%, respectively. The percentage of absorption decreases as time of deposition increases except for the sample dipped for 15 min, which absorbed a higher percentage of radiation than the films deposited for 10 min. The sample coated for 15 min had high density than the sample grew for 10 min.as shown by surface morphological analysis. This could be a reason for the higher absorption of the film deposited for 15 min. It is also seen from the XRD results that the films deposited at 30 and 15 minutes are crystalline while others are amorphous.

Optical band gap

The measured energy gap for ZnS thin films is extrapolated from Fig. 4c and it is in the range of 3.79 to 3.97 eV, which is greater than the bulk energy gap of ZnS of about 3.67 eV. It is observed from the result that the films deposited for 10 and 15 minutes had the same value of 3.90 eV, and the films deposited for 20 and 30 minutes exhibited almost the same band gap of 3.97 eV. A similar higher value of between 3.72 and 3.90 eV was reported (Zhou et al., 2011) who deposited ZnS films by a CBD method at a constant temperature of 80°C and studied the influence of time of deposition between 1 and 3 hours. Also, the results were in line with the reported the energy gap of ZnS thin films coated from acidic solutions at varying deposition temperatures between 55 and 75°C was between 3.75 and 3.88 eV which is also higher than the theoretical band gap of 3.67 eV for ZnS (Abza et al., 2016). The reason for deviation from the bulk energy was attributed to the quantum size effect. However, a wide direct band gap makes thin films a potential application material in optoelectronics devices like solar cells and multilayer dielectric filters because they reduce window absorption losses, which raises the cell's short circuit current.

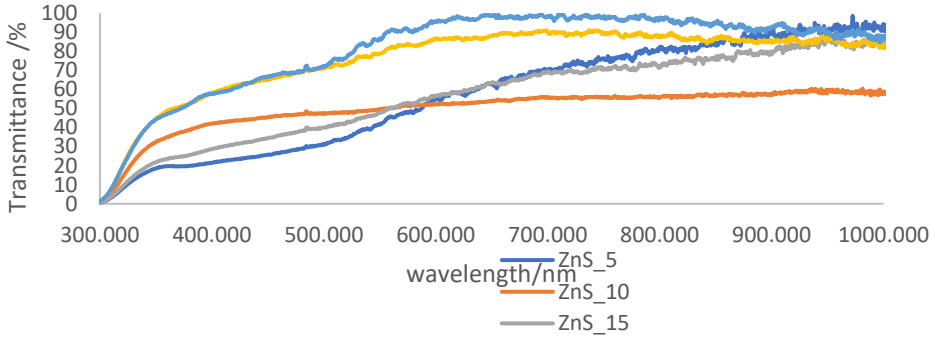

Fig. 4a: Optical transmittance spectra of ZnS at different deposition times

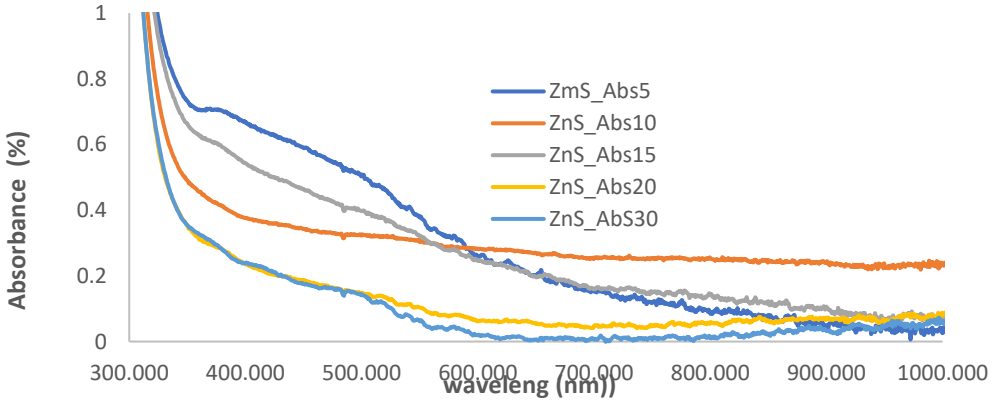

Fig. 4b: Optical absorbance spectra of ZnS at different deposition times

https://doi.org/10.59568/JASIC-2025-6-1-19

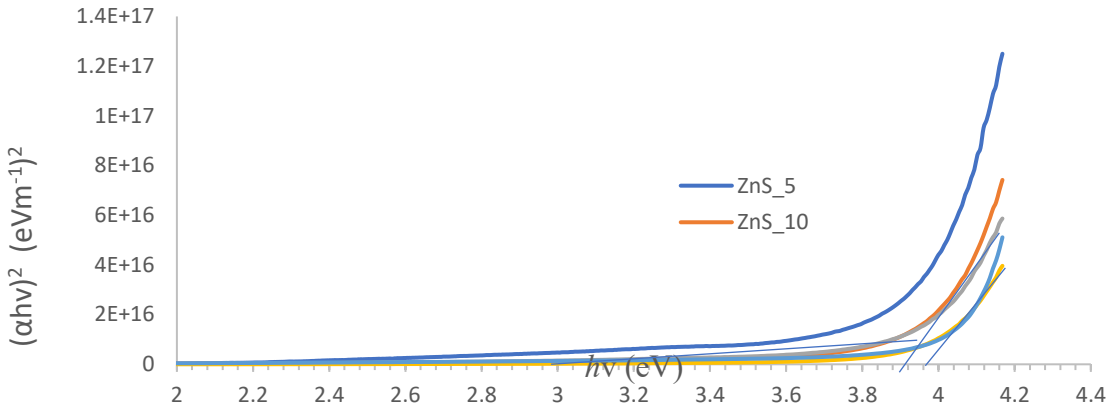

Fig.4c: Graph of hv against $(\alpha hv)^2$ of ZnS thin films deposited at different times

5. Conclusion

The films of ZnS were condensed onto FTO substrates by CBD techniques. The effect of the time of deposition of ZnS on the optical, structural, morphological, and compositional characteristics of the films were investigated. The films have a high transmittance level and low absorbance in the between ultra violet and infrared regions; the extrapolated energy gap was high. The structural properties showed that some of the films were amorphous and some were crystalline. The surface morphology was smooth, and the energy dispersive spectroscopy confirmed the existence of zinc, sulphur, and oxygen with no other impurity atoms. although the EDS shows that the zinc percentage was higher in the films. The films have excellent properties and can take the role of hazardous CdS in thin-film solar cells as a buffer layer.

6. References

[1] Abdullah, H., Saadah, N., & Shaari, S. (2012). Effect of deposition time on ZnS thin films properties by chemical bath deposition (CBD) techinique. *World Applied Sciences Journal*, *19*(8), 1087–1091. https://doi.org/10.5829/idosi.wasj.2012.19.08.591

[2] Abza, T., Ampong, F. K., Hone, F. G., Nkrumah, I., Nkum, R. K., & Boakye, F. (2016). The influence of deposition temperature on the structure and optical band gap of zinc sulphide thin films deposited from acidic chemical baths. *Elixir Condesesed Matter Physics*, *93*, 39511–39514..

[3] Ahn, H., & Um, Y. (2015). Post-annealing effects on ZnS thin films grown by using the CBD method. *Journal of the Korean Physical Society*, *67*(6), 1045–1050. https://doi.org/10.3938/jkps.67.1045

[4] Al-diabat, A. M., Ahmed, N. M., Hashim, M. R., & Almessiere, M. A. (2019). Growth of ZnS Thin Films using Chemical Spray Pyrolysis Technique. *Materials Today: Proceedings*, *17*, 912–920. https://doi.org/10.1016/j.matpr.2019.06.390

[5] Ben Nasr, T., Kamoun, N., Kanzari, M., & Bennaceur, R. (2006). Effect of pH on the properties of ZnS thin films grown by chemical bath deposition. *Thin Solid Films*, *500*(1–2), 4–8. https://doi.org/10.1016/j.tsf.2005.11.030

[6] Chander, A. H., Krishna, M., & Srikanth, Y. (2015). Comparison of Different types of Solar Cells – a Review. *IOSR Journal of Electrical and Electronics Engineering Ver. I*, *10*(6), 151–154. https://doi.org/10.9790/1676-1061151154

[7] Djelloul, A., Adnane, M., Larbah, Y., & Hamzaoui, S. (2016). Morphology , structural and optical study of ZnS thin films prepared by Successive Ionic Layer Adsorption and Reaction (SILAR) Method. *Journal of Optoelectronics and Advanced Materials*, *18*(2), 136–141.

[8] Fluieraru, C. P., Preducă, G., Andrei, H., Diaconu, E., Cotfas, P. A., & Cotfas, D. T. (2019). Determination of Technological Features of a Solar Photovoltaic Cell Made of Monocrystalline Silicon P+PNN+. *International Journal of Photoenergy*, 1–14. https://doi.org/10.1155/2019/7945683

[9] Gułkowski, S., & Krawczak, E. (2017). Experimental studies of thin films deposition by magnetron sputtering method for CIGS solar cell fabrication. *E3S Web of Conferences*, *19*, 0–3. https://doi.org/10.1051/e3sconf/20171903006

[10] Haque, F., Rahman, K. S., Islam, M. A., Rashid, M. J., Alam, M. M., Alothman, Z. A., & Sopian, K. (2014). Growth Optmizatiom of ZnS thin films by RF Magnetron Sputtering as Prospective Buffer Layer in Thin Film Solar Cells. *Chalcogenide Letters*, *11*(4), 189–197.

[11] Hwang, D. H., Ahn, J. H., Hui, K. N., Hui, K. S., & Son, Y. G. (2012). Structural and optical properties of ZnS thin films deposited by RF magnetron sputtering. *Nanoscale Research Letters*, *7*(26), 1–7.

[12] Kawar, S. S., & Pawar, B. H. (2010). Nanocrystalline grain size in ZnS thin films deposited by chemical bath technique. *Journal of Materials Science: Materials in Electronics*, *21*(9), 906–909. https://doi.org/10.1007/s10854-009-0016-z

[13] Kowsar, A., Rahaman, M., Islam, M. S., Imam,

A. Y., Debnath, S. C., Sultana, M., Hoque, M. A., Sharmin, A., Mahmood, Z. H., & Farhad, S. F. U. (2019). Progress in major thin-film solar cells: Growth technologies, layer materials and efficiencies. *International Journal of Renewable Energy Research*, *9*(2), 579–597. https://doi.org/10.20508/ijrer.v9i2.9054.g7628

[14] Kumar, H., & Mahesh, H. (2017). Studies on Optical Properties of ZnS Thin Film by Thermal Evaporation Technique. *International Journal of Advance Research, Ideas and Innovations in Technology*, *3*(1), 97–101.

[15] Manjulavalli, T. E., & Kannan, A. G. (2015). Structural and optical properties of ZnS thin films prepared by chemical bath deposition method. *International Journal of ChemYech Research*, *8*(11), 396–402.

.[16] Nabiyouni, G., Sahraei, R., Toghiany, M., Ara, M. H. M., & Hedayati, K. (2011). Preparation and characterization of nanostructured ZnS thin films grown on glass and N-type Si substrates using a new chemical bath deposition technique. *Reviews on Advanced Materials Science*, *27*(1), 52–57.

[17] Netravati, U. M. & Patil, V. C. (2015). Problems with Non-Renewable Sources: A Survey. International Journal of Advanced Research in Computer Science & Technology 3(1). *International Journal of Advanced Research in Computer Science & Technology*, *3*(1), 2014–2015. www.ijarcst.com

[18] Nikzad, M., Khanlary, M. R., & Rafiee, S. (2019). Structural, optical and morphological properties of Cu-doped ZnS thin films synthesized by sol–gel method. *Applied Physics A: Materials Science and Processing*, *125*(8). https://doi.org/10.1007/s00339-019-2790-7

[19] Osanyinlusi, O. (2020). Preparation and Characterization of ZnS Thin Films Grown by Spin Coating Technique. *Tanzania Journal of Science*, *46*(2), 534–547. https://dx.doi.org/10.4314/tjs.v46i2.28

[20] Rajapakse, R. M. G. (2007). Depletion of nonrenewable energy resources, entropy crisis and nanotechnology solutions. *Journal of the National Science Foundation of Sri Lanka*, *35*(2), 59–61. https://doi.org/10.4038/jnsfsr.v35i2.3669

[21] .Sharma, S., Jain, K. K., & Sharma, A. (2015). Solar Cells: In Research and Applications—A Review. *Materials Sciences and Applications*, *06*(12), 1145–1155. https://doi.org/10.4236/msa.2015.612113

[22] .Shinde, M. S., Ahirrao, P. B., & Patil, R. S. (2011). " Structural , Optical and Electrical Properties of Nanocrystalline ZnS thin films Deposited by Novel Chemical Route ." *Advanced in Appliied Science Research*, *3*(2), 311–317.

[23] Suhail, M. H., & Ahmed, R. A. (2014). Structural , optical and electrical properties of doped copper ZnS thin films prepared by chemical spray pyrolysis technique. *Advanced in Appliied Science Research*, *5*(5), 139–147.

[24] Vishwakarma, R. (2015). Effect of substrate temperature on ZnS films prepared by thermal evaporation technique. *Journal of Theoretical and Applied Physics*, *9*(3), 185–192. https://doi.org/10.1007/s40094-015-0177-5

[25] Wei, A., Liu, J., Zhuang, M., & Zhao, Y. (2013). Materials Science in Semiconductor Processing Preparation and characterization of ZnS thin films prepared by chemical bath deposition. *Materials Science in Semiconductor Processing*, *16*(6), 1478–1484. https://doi.org/10.1016/j.mssp.2013.03.016 thin films performance with chemical bath deposition. *Physics Procedia*, *22*, 354–359. https://doi.org/10.1016/j.phpro.2011.11.055